

# MAGNETIC PROPERTIES OF COMPOSITES OF $\gamma$ -Fe<sub>2</sub>O<sub>3</sub> NANOPARTICLES COVERED BY Me<sub>3</sub>[Fe(CN)<sub>6</sub>]<sub>2</sub>·H<sub>2</sub>O (Me=Co AND Ni)

N. Guskos<sup>1,2</sup>, D. Petridis<sup>3</sup>, S. Glenis<sup>1</sup>, A. Diamantopoulou<sup>1</sup>, J. Typek<sup>2</sup>, A. Guskos<sup>2</sup> and G. Zolnierkiewicz<sup>2</sup>

<sup>1</sup>Department of Solid State Section, Faculty of Physics, University of Athens, Panepistimiopolis, 15 784 Zografos, Athens, Greece

<sup>2</sup>Institute of Physics, West Pomeranian University of Technology, Al. Piastow 48, 70-311 Szczecin, Poland

<sup>3</sup>NCSR „Demokritos“, Aghia Paraskevi, Attikis, Athens, Greece

Received: August 07, 2015

**Abstract.** Magnetic properties of two composites of  $\gamma$ -Fe<sub>2</sub>O<sub>3</sub> (maghemite) nanoparticles covered by molecular magnets of Me<sub>3</sub>[Fe(CN)<sub>6</sub>]<sub>2</sub>·H<sub>2</sub>O (Me(II)=Co and Ni) have been studied. Temperature dependence of magnetic susceptibility in ZFC and FC modes has been obtained for different applied magnetic fields. Additionally, magnetic field dependence of the magnetization has been recorded at different temperatures. For sample with cobalt, no blocking temperature up to 350K was registered in an applied magnetic field of 100 Oe. On the other hand, in 500 Oe the blocking temperature was about 300K. For the system with nickel, the blocking temperature was much lower at high values of applied magnetic field. In both cases, the hysteresis loops have been recorded and the coexistence of ferromagnetic and antiferromagnetic phase has been observed. The antiferromagnetic interactions were stronger for the sample with nickel ions. The presence of stronger antiferromagnetic interaction influenced the coercive field, the remanence field and saturation magnetization. Especially interesting was its influence on the temperature dependences of these parameters.

## 1. INTRODUCTION

Hybrid nanostructures containing two or more nanoscale partners define an important class of materials owing to the potential synergetic effects induced by interactions between these nanometer-scale objects. Such effects could lead to advanced multifunctional materials with a wide technological applications in magnetism, catalysis, energy, electronics etc. In particular, magnetic nanoparticles, due to finite size effects, surface effects and interparticle interactions exhibit quite different magnetic properties from bulk materials. A characteristic example is the exchange anisotropy behavior observed in nanoparticles of a ferromagnetic (FM) cobalt core and an antiferromagnetic (AFM) cobalt oxide shell [1].

On the other side, in seeking selective magnetic nanostructures to develop advanced composite magnetic materials, we turned our attention to the class of molecular magnets and, in particular, to the transition metal cyanide complexes which have been shown to exhibit ferrimagnetic or ferromagnetic coupling. In this context, Prussian Blue analogues play a major role in the field of magnets that order at relatively high temperatures [2]. Moreover, molecular magnets, incorporating hexacyanoferrate anions, exhibit various photomagnetic properties [3].

In this study, we report the synthesis and magnetic behavior of hybrid structures made up of a  $\gamma$ -Fe<sub>2</sub>O<sub>3</sub> (maghemite) core surrounded by a M<sub>3</sub>[Fe(CN)<sub>6</sub>]<sub>2</sub> (M(II)=Ni and Co) molecular magnet. The metal cyanide derivative shows a ferromagnetic

Corresponding author: G. Zolnierkiewicz, e-mail: gzolnierkiewicz@zut.edu.pl

ordering at 14K and 23K for the sample with nickel and cobalt, respectively [5].

## 2. EXPERIMENTAL

All of the starting chemicals were of analytical reagent grade and used as received. Synthesis of hybrid  $\gamma\text{-Fe}_2\text{O}_3/\text{M}_3[\text{Fe}(\text{CN})_6]_2$  ( $\text{M}(\text{II}) = \text{Co}, \text{Ni}$ ) nanocomposites has been done. The synthesis involved the following three steps:

-Synthesis of nano  $\gamma\text{-Fe}_2\text{O}_3$ . This was prepared by oxidation of  $(\text{NH}_4)_2\text{Fe}(\text{SO}_4)_2 \cdot 6\text{H}_2\text{O}$  by hydrogen peroxide in alkaline environment [5].

- The pulp of  $\gamma\text{-Fe}_2\text{O}_3$ , resulting after washing the prepared oxide with water, was dispersed in 30 ml of water.

-The dispersion was treated with small amounts of 2% solution of  $\text{K}_3[\text{Fe}(\text{CN})_6]$ . This treatment brought about "solubilization" of the magnetic oxide dispersion. The resulting mixture was centrifuged at 10000 rpm for ten minutes. The isolated solid was dispersed in 30 ml of water and this dispersion was treated with a solution of  $\text{Co}(\text{II})$  or  $\text{Ni}(\text{II})$  salt. The composites were isolated by centrifugation, washed with water and air dried.

DC magnetization measurements were carried out with a MPMS-7 SQUID magnetometer in the temperature range of 2-350K and magnetic fields up to 70 kOe in the zero-field-cooling (ZFC) and field cooling (FC) modes.

## 3. RESULTS AND DISCUSSION

Figs. 1 and 2 present the temperature dependence of the nanocomposites  $\gamma\text{-Fe}_2\text{O}_3/\text{Co}_3[\text{Fe}(\text{CN})_6]_2$  (sample 1) and  $\gamma\text{-Fe}_2\text{O}_3/\text{Ni}_3[\text{Fe}(\text{CN})_6]_2$  (sample 2) magnetization in ZFC and FC modes, registered in different values of applied magnetic fields.

Sample 1 exhibits no blocking temperature up to 350K in an applied magnetic field of 100 Oe. Only above 500 Oe does the maximum value of magnetization at the ZFC mode begins to appear. In high magnetic fields, a broad, field dependent peak is observed in the ZFC magnetization curve at  $T_{\text{max}}$  for both samples. In the case of non-interacting nanoparticles,  $T_{\text{max}}$  marks the average blocking temperature of the superparamagnetic moments at the time scale of the measurement, depending on the particle-size distribution [6,7]. The dipolar and exchange interactions between nanoparticles could be responsible for the shift of  $T_{\text{max}}$  towards higher temperatures as well as the broadening of the  $M_{\text{ZFC}}$  peak and flattening of the ZFC/FC curves above  $T_{\text{max}}$ , pointing to a dominant magnetic interaction effect [8,9].

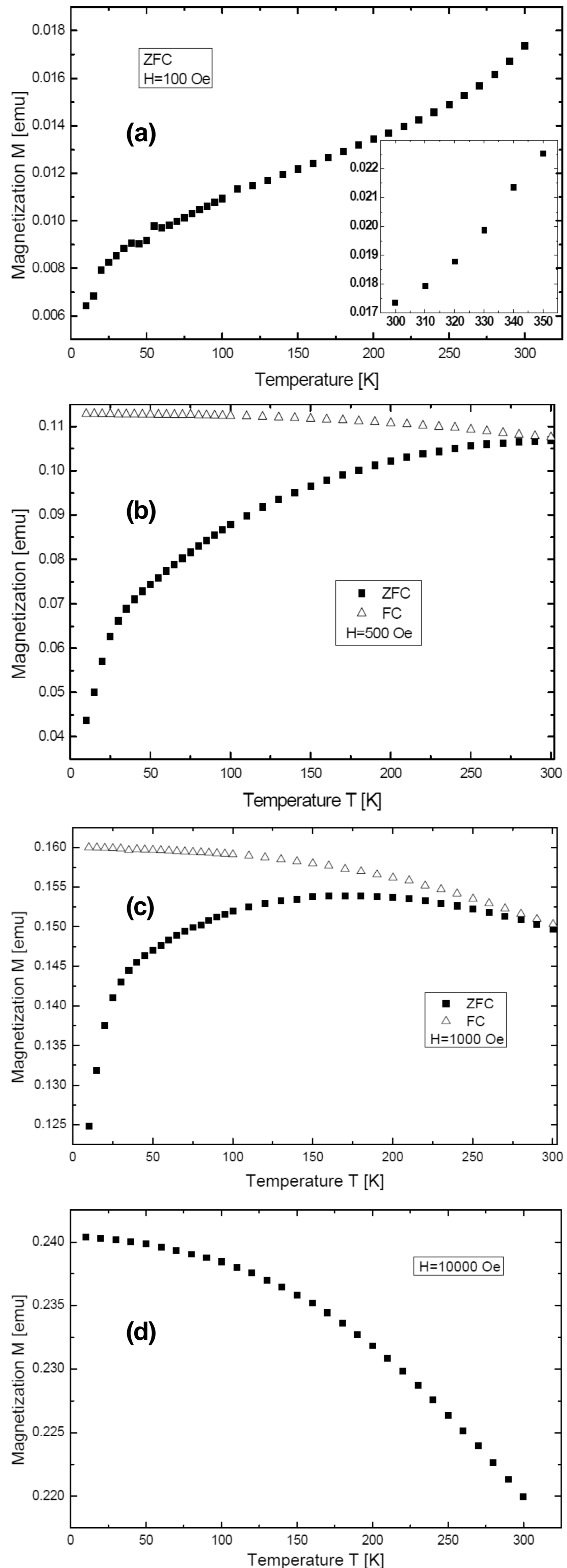


**Fig. 1.** Temperature dependence of the magnetization of sample  $\text{Fe}_2\text{O}_3/\text{Co}_3[\text{Fe}(\text{CN})_6]_2$  ( $m = 2.9$  mg) in ZFC and FC modes using different applied magnetic fields; (a)  $H = 100$  Oe, (b)  $H = 500$  Oe, (c)  $H = 1$  kOe and (d)  $H = 10$  kOe.

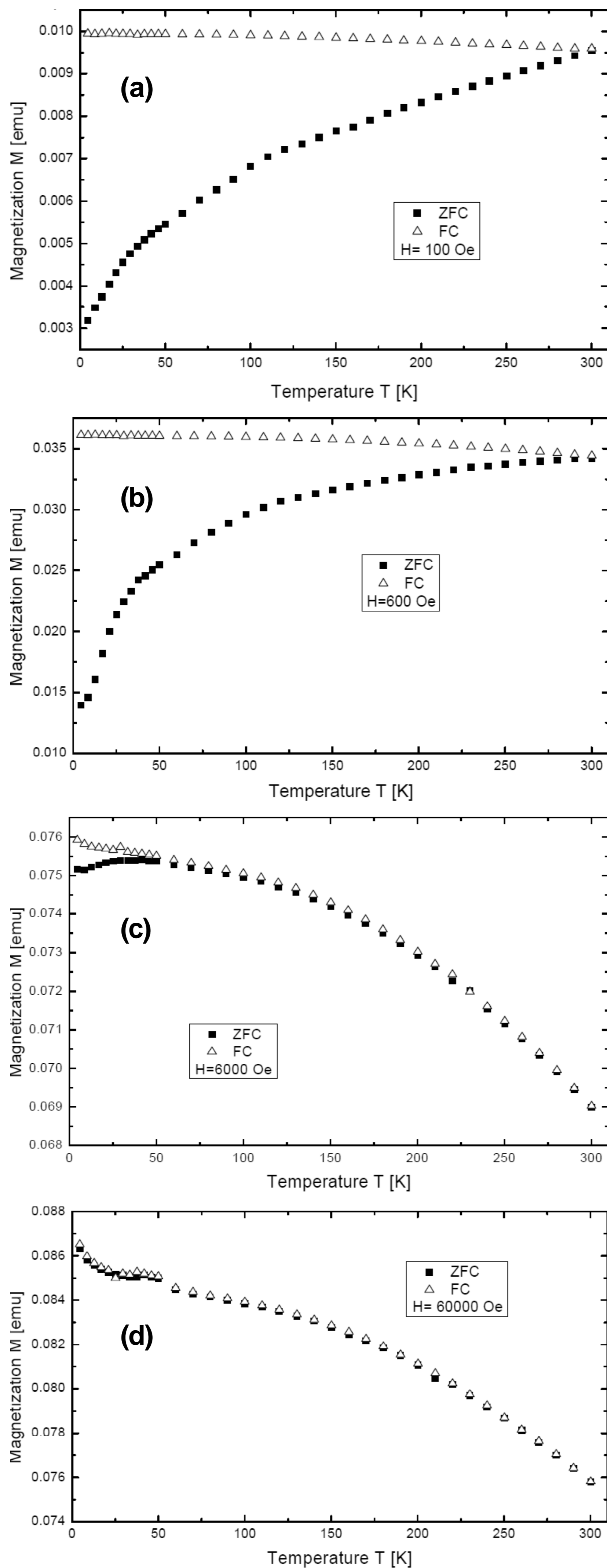


**Fig. 2.** Temperature dependence of the magnetization of sample  $\text{Fe}_2\text{O}_3/\text{Ni}_3[\text{Fe}(\text{CN})_6]_2$  in ZFC and FC modes using different applied magnetic fields ( $m = 2.6$  mg); (a)  $H = 100$  Oe, (b)  $H = 500$  Oe, (c)  $H = 6$  kOe and (d)  $H = 60$  kOe.

Fig. 3 shows the temperature dependence of the inverse magnetization ( $M^{-1}$ ), obtained from FC mode measurements at 60 kOe for both samples. A Cu-

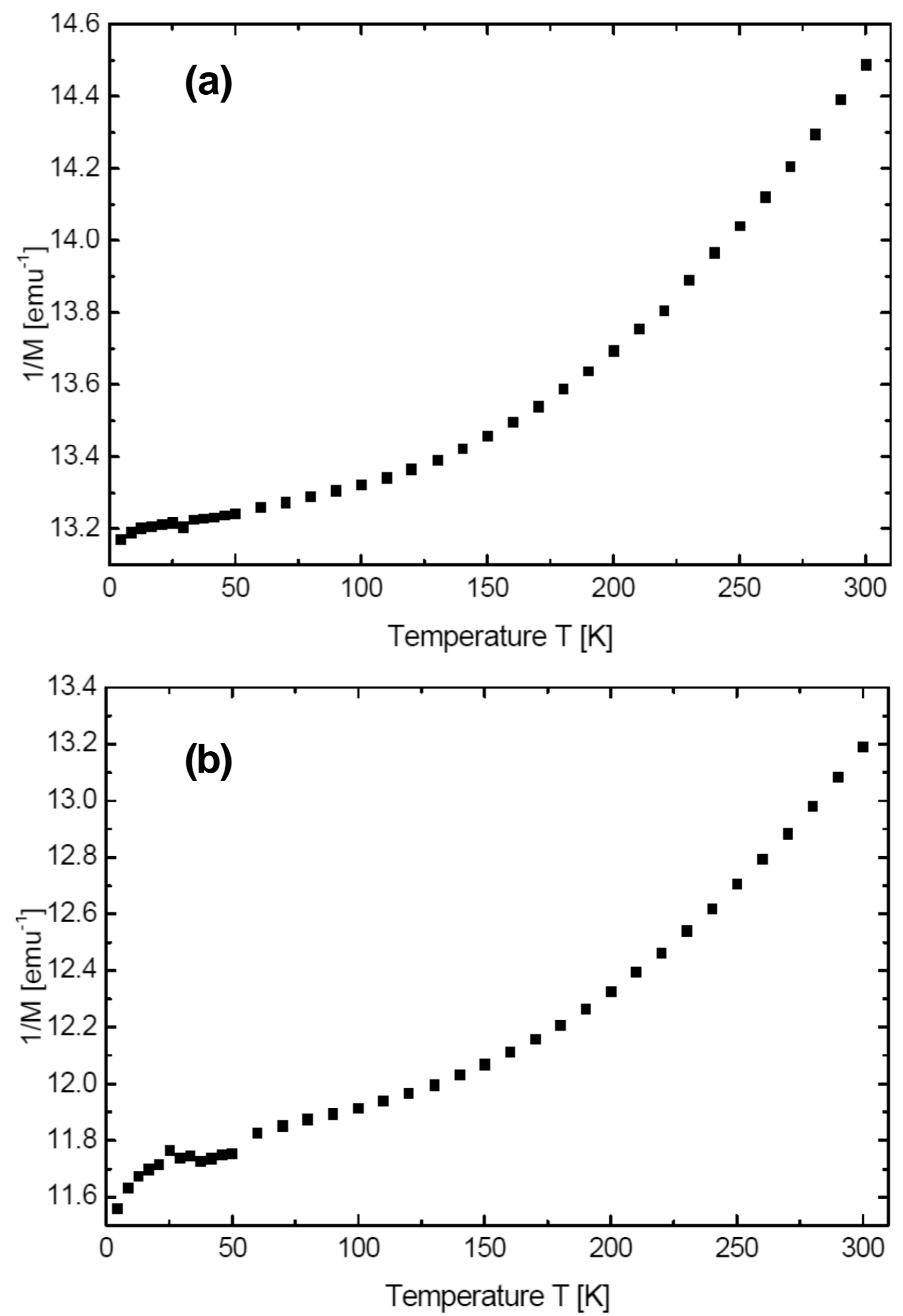


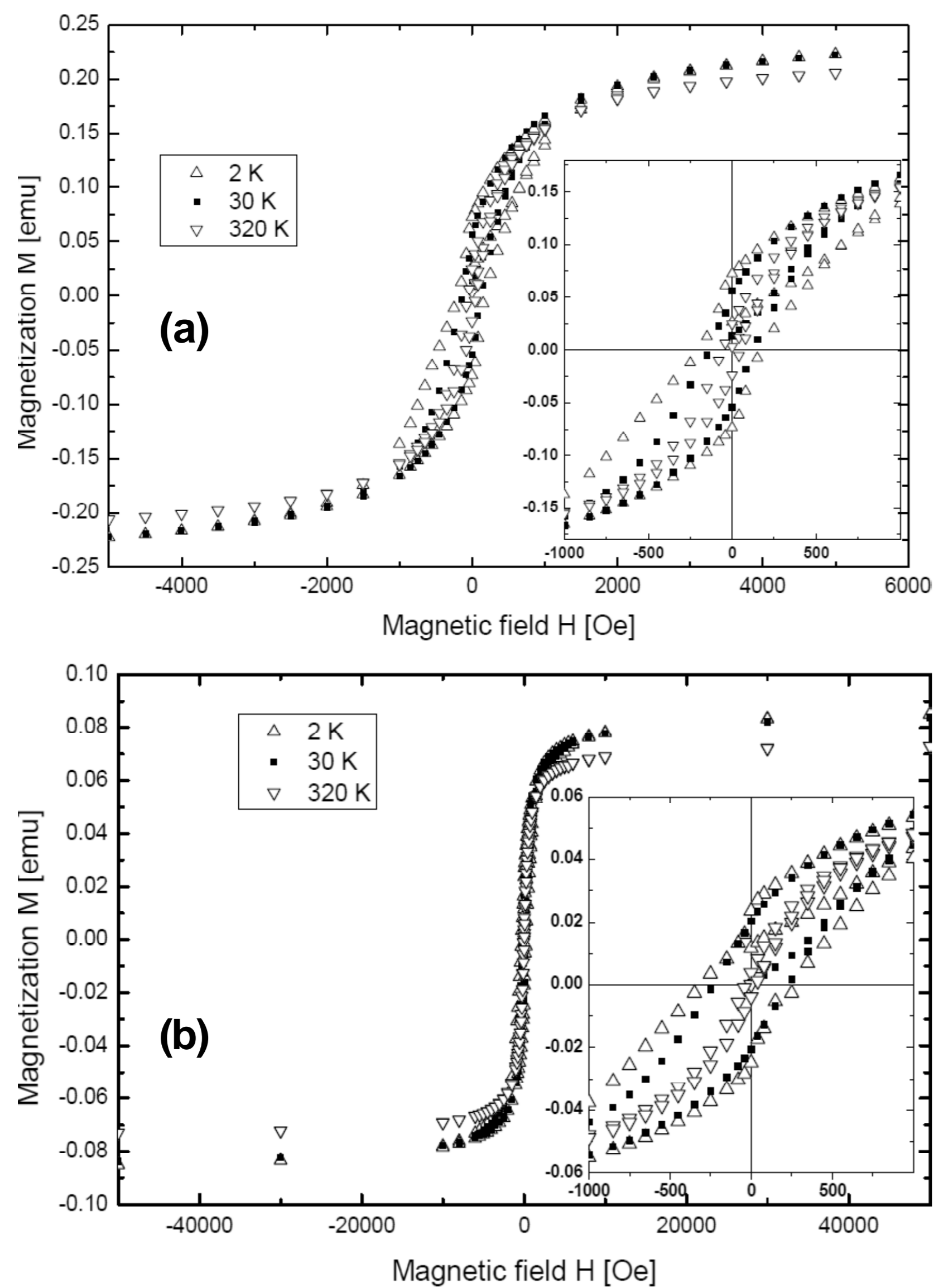
**Fig. 3.** Temperature dependence of the inverse magnetization for the compounds: a)  $\text{Fe}_2\text{O}_3/\text{Co}_3[\text{Fe}(\text{CN})_6]_2$  and b)  $\text{Fe}_2\text{O}_3/\text{Ni}_3[\text{Fe}(\text{CN})_6]_2$ .

rie-Weiss type behavior prevails in both high and low temperature ranges. The Curie-Weiss fit of  $M(T)^{-1}$  to the experimental data at  $T > 230$  K allows the determination of the Curie-Weiss temperature ( $\Theta$ ). At high temperature ranges, the value of  $\Theta$  is calculated to be positive, whereas, at low temperatures, this value is negative, suggesting the coexistence of ferromagnetic and antiferromagnetic interactions (Table 1) in both test systems. At low temperatures, a spin correlated state is observed in both cases, but it is stronger for sample 2 (Table 1).

Fig. 4 shows the hysteresis loops for the two studied samples measured at different temperatures. Both loops exhibit a similar shape. This shape is also similar to that for low concentrations of  $\gamma\text{-Fe}_2\text{O}_3$  magnetic nanoparticles embedded in nanocomposite [10,11]. Some differences in the hysteresis-loop shift are observed. These differences could arise when a ferromagnet (FM) coexists with an antiferromagnet (AFM) [12-14]. Magnetic exchange interaction between FM and AFM states could form additional anisotropy, as the presence of an exchange bias magnetic field in nanosize magnetic particles could provide higher blocking

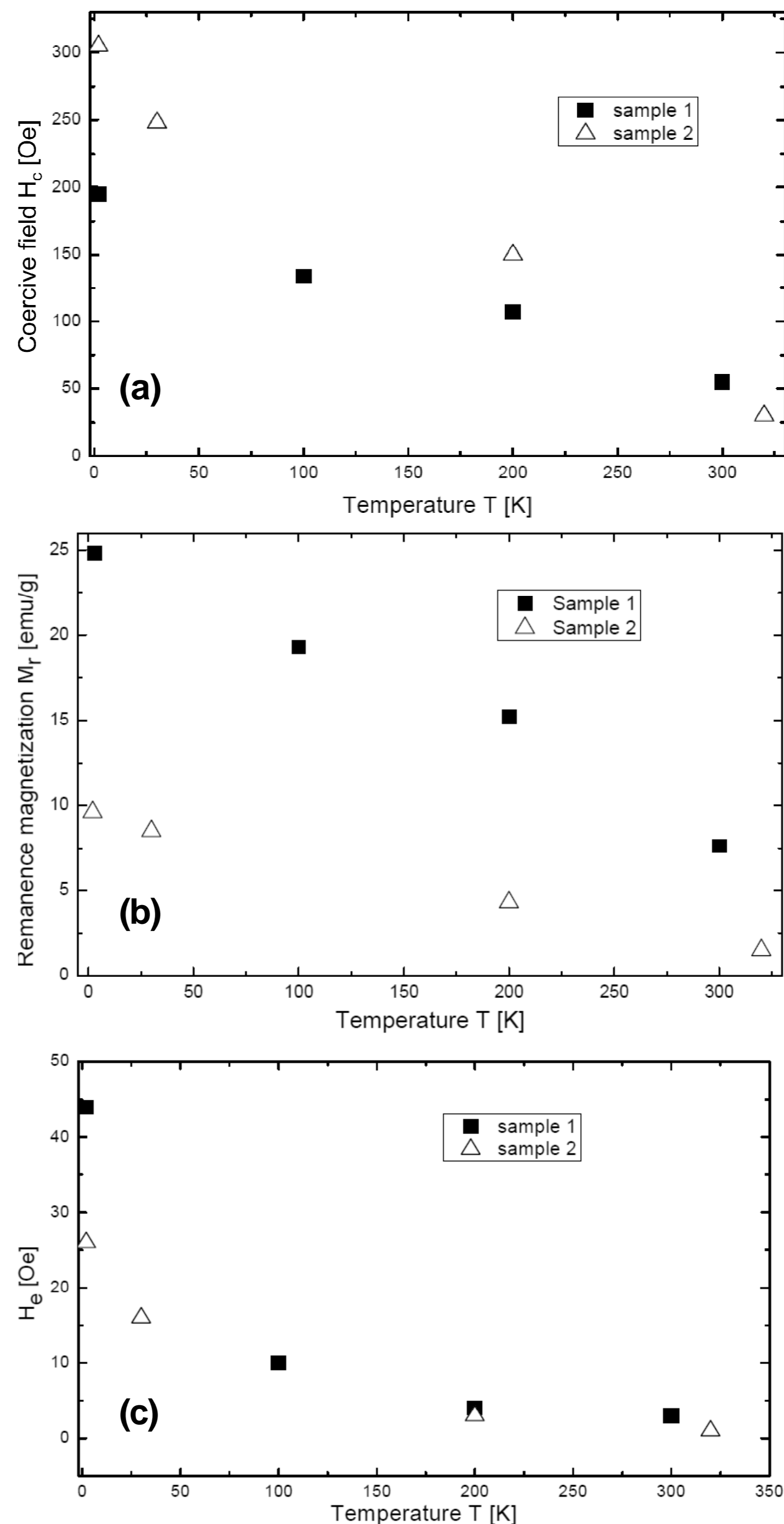
**Table 1.** Values of the Curie-Weiss temperature  $\Theta$  obtained in different temperature ranges  $\Delta T$  and transition temperature to ordered magnetic state  $T_N$ .

	$\Delta T$ [K]	$\Theta$ [K]	$\Delta T$ [K]	$\Theta$ [K]	$T_N$ [K]
Sample 1	230-300	160(2)	40 - 60	-61(3)	5
Sample 2	230-300	140(2)	10 - 100	-86(3)	24

**Fig. 4.** Magnetic field dependence of the magnetization of the compounds: a)  $\text{Fe}_2\text{O}_3/\text{Co}_3[\text{Fe}(\text{CN})_6]_2$  and b)  $\text{Fe}_2\text{O}_3/\text{Ni}_3[\text{Fe}(\text{CN})_6]_2$ .

temperature ( $T_B$ ) and coercive field ( $H_c$ ) [15]. The exchange-bias field ( $H_e$ ) is defined as the offset of the hysteresis loop along the field axis  $H_e = (H_+ + H_-)/2$ , where  $H_+$  and  $H_-$  are the intersections on the field axis at increasing and decreasing fields in the FC hysteresis loop, and the coercive field ( $H_c$ ) as half of its width,  $H_c = (H_+ - H_-)/2$  [14].

Fig. 5 presents the temperature dependence of the coercive field ( $H_c$ ), remanence ( $M_r$ ) and the exchange bias field ( $H_e$ ) for both systems. An almost linear behavior is observed for the  $H_c$ . At low temperatures, the value of the coercive field  $H_c$ , obtained for sample 2 ( $H_c = 300$  Oe) is greater than the corresponding value of sample 1 ( $H_c = 200$  Oe), whereas, at higher temperatures, the opposite behavior is recorded ( $H_c = 20$  Oe and 50 Oe, respectively). The value of the ratio  $\Delta H_c/\Delta T$  is  $\Delta H_c/\Delta T = 0.45(5)$  Oe/K

**Fig. 5.** Temperature dependence of a)  $H_c$ , b)  $M_r$  and c)  $H_e$ .

and  $\Delta H_c/\Delta T = 0.80(8)$  Oe/K for system 1 and system 2, respectively. The remanence field ( $M_r$ ) is approximately 25% for sample 1 and 30% for sample 2 at low temperatures, which is quite lower than the theoretical value of about 50%, predicted for an assembly of non-interacting uniaxial single domain particles with randomly oriented anisotropy axes. An almost linear behavior is recorded for the remanence

for both systems, with the ratio  $\Delta M_r/\Delta T$  acquiring the following values:  $\Delta M_r/\Delta T = 5.8 \cdot 10^{-2}$  emu/(g·K) for sample 1 and  $\Delta M_r/\Delta T = 2.5 \cdot 10^{-2}$  emu/(g·K) for sample 2. This ratio is two times higher for sample 1.

The saturation of magnetization is over two times greater for system 1. Nickel ions, in the presence of iron ions, can form complicated magnetic states [16,17]. There are strong antiferromagnetic interaction, hence many of them can be interchangeably coupled up to high temperatures.

#### 4. CONCLUSIONS

The sample with cobalt ions (sample 1) exhibited higher blocking temperatures. The sample with nickel ions (sample 2) demonstrated stronger antiferromagnetic coupling. The coexistence of ferromagnetic and antiferromagnetic interactions formed an anisotropy hysteresis loop, which almost disappeared for sample 2 in the high temperature range. The presence of stronger antiferromagnetic interactions in the system with nickel ions influenced the coercive field. At low temperatures, the value of  $H_c$  in sample 2 was higher than the corresponding value of sample 1, but it decreased more rapidly with increasing temperature. The remanence field was higher at low temperatures for the system with cobalt ions and decreased more rapidly with increasing temperature.

#### REFERENCES

- [1] S. B. Darling and S. D. Bader // *J. Mater. Chem.* **15** (2005) 4189.
- [2] J. V. Barth, G. Costantini and K. Kern // *Nature* **437** (2005) 671.
- [3] C. Wang, L. Yin, L. Zhang, L. Kang, X. Wang and R. Gao // *J. Phys. Chem. C* **113** (2009) 4008.
- [4] A. Jain, M. Jamet, A. Barski, T. Devillers, I.S. Yu, C. Porret, P. Bayle-Guillemaud, V. Favre-Nicolin, S. Gambarelli, V. Maurel, G. Desfonds, J. F. Jacquot, and S. Tardif // *J. Appl. Phys.* **109** (2011) 013911
- [5] S. Juszczak, C. Johansson, M. Hanson, A. Ratuszna and G. Malecki // *J. Phys.: Condens. Matter* **6** (1994) 5697.
- [6] J. L. Dormann, D. Fiorani and E. Tronc // *Adv. Chem. Phys.* **98** (1997) 283.
- [7] P.P. Vaishnava, U. Senaratne, E.C. Buc, R. Naik, V.M. Naik, G.M. Tsoi and L.E. Wenger // *Phys. Rev. B* **76** (2007) 024413.
- [8] R. W. Chantrell, N. S. Walmsley, J. Gore and M. Maylin // *Phys. Rev. B* **63** (2000) 024410.
- [9] C. Binns, M. J. Maher, Q. A. Pankhurst, D. Kechrakos and K. N. Trohidou // *Phys. Rev. B* **66** (2002) 184413.
- [10] N. Guskos, V. Likodimos, S. Glenis, J. Typek, M. Maryniak, Z. Roslaniec, M. Baran, R. Szymczak, D. Petridis and M. Kwiatkowska // *J. Appl. Phys.* **99** (2006) 084307.
- [11] N. Guskos, V. Likodimos, S. Glenis, M. Maryniak, M. Baran, R. Szymczak, Z. Roslaniec, M. Kwiatkowska and D. Petridis // *J. Nanosci. Nanotech.* **8** (2008) 2127.
- [12] C. Martínez-Boubeta, K. Simeonidis, M. Angelakeris, N. Pazos-Perez, M. Giersig, A. Delimitis, L. Nalbandian, V. Alexandrakis and D. Niarchos // *Phys. Rev. B* **74** (2006) 054430.
- [13] A. Shavel, B. Rodríguez-Gonzalez, M. Spasova, M. Farle and L. M. Liz-Marzan // *Adv. Funct. Mater.* **17** (2007) 3870.
- [14] R. Chalasani and S. Vasudevan // *J. Phys. Chem. C* **115** (2011) 18088.
- [15] V. Skumryev, S. Stoyanov, Y. Zhang, G. Hadjipanayis, D. Givord and J. Nogues // *Nature* **423** (2003) 850.
- [16] N. Guskos, J. Typek, G. Zolnierkiewicz, A. Blonska-Tabero, M. Kurzawa, S. Los and W. Kempinski // *Materials Science-Poland* **24** (2006) 983.
- [17] N. Guskos, V. Likodimos, S. Glenis, J. Typek, J. Majszczyk, G. Zolnierkiewicz, A. Blonska-Tabero and C. L. Lin // *Rev. Adv. Mat. Sci.* **14** (2007) 85.